Print ISSN 2710-0952   Electronic ISSN 2790-1254

Experimental and Numerical Investigation of a Solar-Powered Desalination System"

Samah Mohammed Abed

Abstract

Both theoretical and experimental studies of a solar-powered desalination unit are presented in this paper. To increase the system's thermal efficiency, a modification module was included. This upgrade consists of a simple serpentine-style heat exchanger and a solar parabolic trough collector with a focus pipe.. Thermal oil is selected as the heat transfer medium due to its favorable thermo physical properties. The oil circulates in a closed-loop path between the focal pipe and the serpentine exchanger.The enhancement unit operates both during daylight hours and at night. Throughout the day, the oil is heated by direct solar irradiation and concentrated thermal energy collected by the solar trough. The parabolic collector is equipped with a simple sun-tracking mechanism to maximize solar capture through optimal angular orientation. A transparent plastic cover encloses the collector to minimize convective heat loss to the environment, thereby utilizing the greenhouse effect.The serpentine heat exchanger, made of copper and coated in black for better heat absorption, is installed at the base of the solar still's basin. Thermally insulated pipelines connect it to the parabolic trough, ensuring minimal thermal losses. A small pump, potentially powered by a photovoltaic (PV) system, drives the circulation of the thermal oil.Saline water within the basin is heated both by direct sunlight and indirectly by means of thermal conduction from the heated oil that is circulating inside the exchanger. Using the energy balance equations for each key component, a thorough thermal study of the complete system is performed. The pump's performance attributes and the driving motor's parameters are also recorded. The improved system's total effectiveness is calculated and evaluated..Two experimental trials were conducted in April and June 2005. Measurements of key temperature points across the system were recorded using Type-K thermocouples (±0.5°C), a digital temperature monitoring device, and a remote control system. Meteorological data for the selected testing days were sourced from the "Egyptian Solar Radiation Atlas," published by the Geophysical Institute.The performance of the enhanced system is compared with that of a conventional solar desalination setup. An economic evaluation of the upgraded system is also included. Results indicate that freshwater output the implemented modifications.

Keywords: Forced circulation; Passive flow; Oil-based heat exchanger; Parabolic solar collector; Miniature .

العـــــدد 19A تشر2ين 2025 المجلة العراقية للبحوث الإنسانية والإجتماعية والعلمية
No.19A Nov. 2025 Iraqi Journal of Humanitarian, Social and Scientific Research
Print ISSN 2710-0952 Electronic ISSN 2790-1254

التحقيق التجريبي والعددي لنظام تحلية يعمل بالطاقة الشمسية

سماح محمد عبد

الملخص:

يقدّم هذا البحث دراسة نظرية وتجريبية لوحدة تحلية تعمل بالطاقة الشمسية، وقد أُجريت تعديلات هندسية لزيادة الكفاءة الحرارية للنظام. تضمّن التعديل إضافة وحدة تحسين تتألف من مبادل حراري على شكل أنبوب حلزوني (Serpentine) ومجمّع شمسي على شكل القطع المكافئ (Parabolic Trough Collector) مزوّد بأنبوب بؤري.تم اختيار الزيت الحراري كوسط ناقل للحرارة نظرًا لخواصه الثرموفيزيائية الملائمة. يدور الزيت في مسار مغلق بين الأنبوب البؤري والمبادل الحراري الحلزوني. تعمل وحدة التحسين خلال ساعات النهار والليل على حد سواء؛ إذ يُسخَّن الزيت أثناء النهار بواسطة الإشعاع الشمسي المباشر والطاقة الحرارية المركّزة التي يجمعها المجمّع الشمسي المكافئ. ولتحقيق أعلى كفاءة في جمع الإشعاع، زُوّد المجمّع بآلية تتبّع شمسي بسيطة تعمل على ضبط زاوية التوجيه المثلى. كما غُطِّي المجمّع بغطاء بلاستيكي شفاف للحد من فقدان الحرارة بالحمل إلى البيئة الخارجية، مستفيدًا من تأثير الاحتباس الحراري.المبادل الحراري الحلزوني المصنوع من النحاس والمطلي باللون الأسود لتحسين امتصاص الحرارة ثُبّت في قاعدة حوض جهاز التحلية الشمسي. وقد رُبط المبادل بالمجمّع المكافئ بواسطة أنابيب معزولة حراريًا لتقليل الفواقد الحرارية إلى أدنى حد. ويُستخدم مضخّة صغيرة – يمكن تشغيلها عبر نظام كهروضوئي (– PV)لضمان دوران الزيت الحراري داخل النظام. يُسخَّن الماء المالح في الحوض بطريقتين: التسخين المباشر بواسطة أشعة الشمس، والتسخين غير المباشر عبر التوصيل الحراري من الزيت الساخن الجاري داخل المبادل الحراري. وقد أُجريت دراسة حرارية متكاملة للنظام استنادًا إلى معادلات توازن الطاقة لكل مكوّن رئيسي. كما جرى تسجيل خصائص أداء المضخة ومعلمات المحرك المحرّك لها. وفي النهاية، تم حساب وتقييم الكفاءة الكلية للنظام بعد التعديل. نُفّذت تجربتان عمليتان في شهري نيسان (أبريل) وحزيران (يونيو) من عام 2005. وقد جرى قياس درجات الحرارة في النقاط الرئيسة للنظام باستخدام حساسات نوع (K-Type Thermocouples)بدقة ±0.5°C، وجهاز رقمي لمراقبة الحرارة، ونظام تحكم عن بُعد. أما البيانات المناخية لأيام الاختبار المختارة فاستُقيت من «أطلس الإشعاع الشمسي المصري» الصادر عن المعهد الجيوفيزيائي. تمت مقارنة أداء النظام المطوَّر بأداء نظام تحلية شمسي تقليدي، مع تضمين تقييم اقتصادي للوحدة المعدَّلة. أظهرت النتائج أن كمية المياه العذبة المنتجة ازدادت بفضل التعديلات المنفّذة.

الكلمات المفتاحية: الدوران القسري؛ التدفق السلبي؛ المبادل الحراري المعتمد على الزيت؛ المجمّع الشمسي المكافئ؛ نظام التحلية المصغّر.

1. Introduction

Water scarcity is a pressing concern in arid and coastal regions, where saline or brackish water is abundant but freshwater is limited. Solar desalination offers a cost-effective and sustainable solution for such environments. Egypt, with its high solar radiation intensity and availability, is particularly suitable for solar thermal technologies.

In Gaza, Palestine,. [1] demonstrated a solar-powered performance. By creating a, Klemens et al. [2] were able to produce 50.2 liters of distilled water per day, or 25 L/m², when using 4.8 kWh/m² of solar input per day. In their analysis of a unique desalination technique powered by,. [3] reported an output of 6.5 kg/m²/day, which is much greater than the 3–4 kg/m²/day typical of conventional stills..

In another study, Klemens et al. [4] investigated a tower using flat-plate collectors. Their six-stage design, each with three trays, yielded a water production rate of 1.49 L/kWh·m² — 2.67 times greater than traditional tank-type distillers. Howa [5] and Ghoraba [6] also contributed theoretical and experimental insights into heat and mass transfer in single-slope solar stills.

In the current is harnessed using a system and heat transfer pipelines. Oil is utilized as the within the serpentine exchanger and piping network to enhance thermal performance. The study presents both practical experiments and a comprehensive theoretical assessment to validate the system's improved efficiency

2. Experimental work

Two solar desalination experimental setups

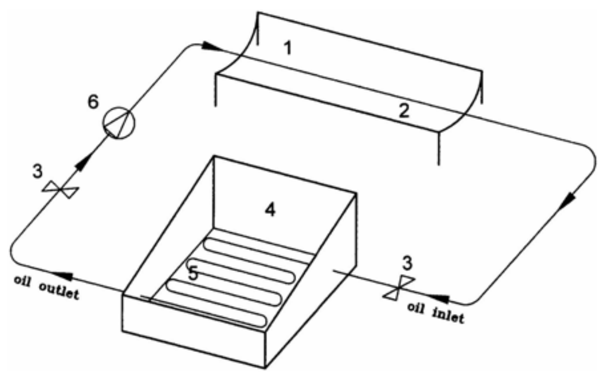

Fig. 1. Experimental set-up of the modified system. 1 parabolic trough, 2 oil pipeline, 3 valves, 4 solar still, 5 oil serpentine, 6 pump.

2. Experimental Setup and System Description

Two solar desalination systems were constructed for comparative analysis: a conventional baseline unit and a second system incorporating the proposed design enhancement. Figures 1–4 illustrate both schematic diagrams and photographic documentation of the experimental setup used in this study.

Two experimental trials were conducted in April and June 2005, focusing on the case study involving forced oil circulation. System temperature measurements were carried out using Type-K thermocouples (accuracy ±0.5°C), a digital temperature measurement device, and a remote monitoring unit. Forecasted weather data, representing Atlas, published by the Geophysical Institute, provided the typical climate for the Cairo test location for the experimental periods (see Figures 5–8). Two solar desalination experimental setups [7].

2.1 Geometric and Functional

The solar parabolic trough collects thermal energy and serves as a concentrator and reflector. It was made from grade 304 stainless steel sheet that was 80 cm long and 0.4 mm thick. To absorb the concentrated sun energy, a 7/8-inch-diameter copper pipe is placed exactly along the parabolic profile's focal axis. The geometric profile of the parabolic collector used in this configuration is shown in Figure 9.

Additionally, a secondary insulated using fiberglass material, is incorporated into the system to facilitate the oil circulation loop. These components collectively form the closed-loop oil cycle, designed to enhance heat transfer efficiency within the desalination system

.

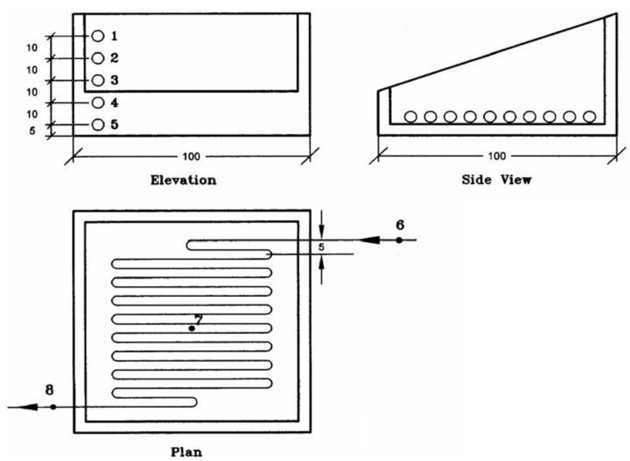

Fig. 2. Thermocouple locations. 1 glass cover temperature, 2 dry bulb temperature 3 wet bulb temperature, 4 surface water temperature, 5 basewater temperature, 6 oil inlet temperature, 7 oil temperature insideserpentine, 8 oil outlet temperature. (Dimensions in cm.)

Print ISSN 2710-0952 Electronic ISSN 2790-1254

Fig. 3. Modified and standard solar stills.

The serpentine loop functions as a basic heat exchanger and is securely wrapped in a layer of insulating wool. This heat exchanger is situated at the solar still's base. To optimize the absorption of incident solar radiation during daylight hours, black paint is applied to the inside walls of the basin as well as the serpentine copper pipe. The working fluid is thermal oil, which is powered by a tiny pump and circulates through the closed loop via forced convection

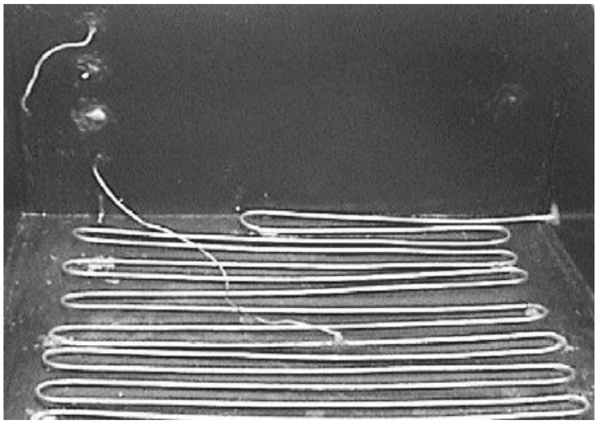

Fig. 4. Serpentine (heat exchanger)

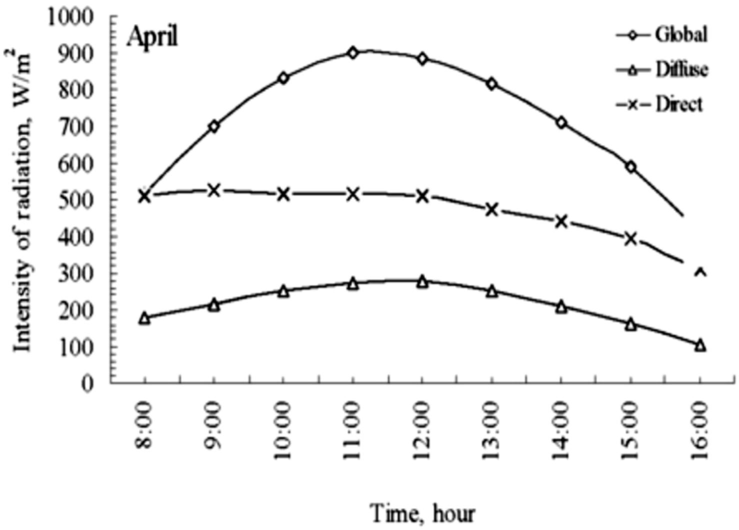

Fig. 5. Solar intensity of Cairo site in April.

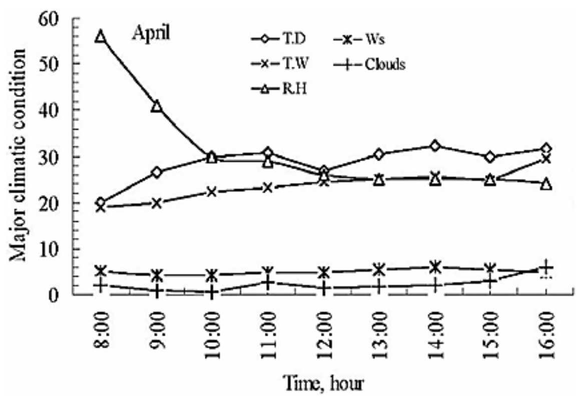

Fig. 6. Climatic conditions of Cairo site in April.

$$CR_o = \frac{\frac{1}{A_r}\int I_r \, d A_r}{I_a} \quad (1)$$

$$CR_g = \frac{A_a}{A_r} \quad (2)$$

In this case, IrI_ stands for the mean stand for the aperture area and receiver surface area of the collector, respectively, measured in square meters; d and f stand

العـــدد 19A تشر2ين 2025
No.19A Nov. 2025
المجلة العراقية للبحوث الإنسانية والإجتماعية والعلمية
Iraqi Journal of Humanitarian, Social and Scientific Research
Print ISSN 2710-0952 Electronic ISSN 2790-1254

for the trough's aperture diameter and focal length, respectively, in meters. The formula used to describe the parabola mathematically is

expressed as follows: $$A_a = L \times d \quad (3)$$

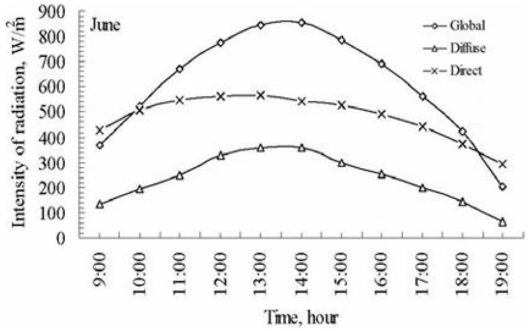

Fig. 7. Solar intensity of Cairo site in June

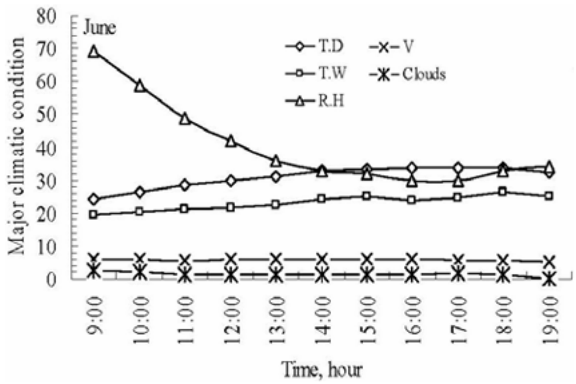

Fig. 8. Climatic conditions of Cairo site in June.

$$A_r = \frac{2}{3} d \times h \quad (4)$$

Where hhh represents the height of the parabola, expressed in relation to the. The aperture diameter refers to the span across the parabola's opening, while the focal length is the distance from the vertex to the focus. The height hhh can be calculated using the following expression::

$$h = \frac{d^2}{16 \; f} \quad (5)$$

Print ISSN 2710-0952 Electronic ISSN 2790-1254

The equation of the parabola symmetric about the x-axisin polar coordinates is as follows, assuming parabola's vertex VVV and that the x-axis coincides with the parabola's axis of symmetry

$$y^2 = 4\,fx \qquad (6)$$

where the distance (VF) between the vertex and the focus is represented by the focal length (f).

$$\frac{4\ f}{r} = \frac{\sin^2\theta}{\cos\theta} \qquad (7)$$

where θ\thetaθ indicates the angle between the x-axis and the radius vector r, and r is the radial distance from the origin. Table 1 displays the physical and thermal properties of the working fluids used in the system

2.4. Motor Specifications

The essential operating parameters of the motor used in the system are as follows:

- **Current (I):** 10 A
- **Voltage (V):** 38 V
- **Output Power (P):** 0.65 HP (approximately 0.5 kW)
- **Armature Resistance (R):** 0.1 Ω
- **Angular Speed (ω_m):** 100 rad/s (equivalent to 958 rpm)

The following relation can be used to calculate the parabolic radius rPr_PrP (in meters), which defines the curvature of the parabolic trough :

$$r_P = \frac{2\ f}{1 + \cos\psi} \qquad (8)$$

Print ISSN 2710-0952 Electronic ISSN 2790-1254

where ψ = 2P represents a close examination of the geometry seen in Fig. 9.
2.3. Specifications for oil

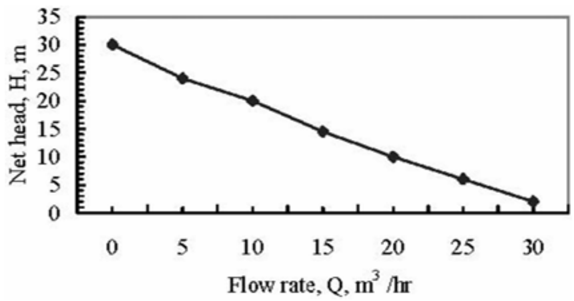

Fig. 10. Performance curve for a pump

Table 1 The chosen fluids' thermal characteristics at 20EC

Fluid	ρ (kg/m^3)	C_p (kJ/kg.k)	η (N.s/m^2)	K (kJ/m.s.k)
Oil	850	1.966	0.0686	0.00014
Water	1000	4.18	—	0.026

Thermo physical Properties
Table 1 provides a summary of the physical and thermal characteristics of the working fluids chosen for the system .

2.4. Motor Specifications

The electrical and mechanical parameters of the motor utilized in the system are listed below:

- **• Current of electricity (I): 10 A**
- **38 V is the voltage supply (V), and 0.65 horsepower (or around 0.5 kW) is the output power (P).**
- **Rotary speed (ω_m): 100 rad/s;**

Print ISSN 2710-0952 Electronic ISSN 2790-1254

(equivalent to 958 revolutions per minute)

2.5. Pump Specifications

The technical characteristics of the pump employed for forced oil circulation are as follows:

• Two meters is the net head (H).
• 28 meters is the maximum head (H_{max}).
• 8 meters is the maximum suction height (S_{max}).

Toughness (τ): 2.4 N/m
• The rotational speed (ω_p) is 120 rad/s, or 1150 rpm.
• Speed ratio (r): ω¯pω¯m=1.2\frac{\bar{\omega}_p}{\bar{\omega}_m} = 1.2ω¯mω¯p=1.2 • Volumetric flow rate (Q): 0.38×10^{-2} m³/s

The pump's operational performance curve is illustrated in Figure 10.

3. Thermal Analysis of the Solar Desalination System

At any given moment, the solar still produces a specific quantity of distilled water, denoted as Wp (in liters per square meter of glass cover area). The corresponding average temperatures for the surrounding ambient air are represented by Tw , Tg , and To (all in °C), respectively. The solar irradiance received by the still is denoted by III (W/m²).

The thermal behavior and energy dynamics of the desalination system are modeled using a series of heat balance equations that account for the energy interactions within each component.

3.1. Thermal Energy Balance of the Glass Cover (qgq_gqg)

The total thermal energy transfer associated with the glass cover is expressed through the following energy balance equation:

المجلة العراقية للبحوث الإنسانية والإجتماعية والعلمية
Iraqi Journal of Humanitarian, Social and Scientific Research
Print ISSN 2710-0952 Electronic ISSN 2790-1254

$$q_g = \alpha_g I - q_{Lg}, \text{ W/m}^2 \quad (9)$$

where

$$q_{Lg} = q_{cg} + q_{rg}, \text{ W/m}^2 \quad (10)$$

$$q_{cg} = h_{cg} (T_g - T_o), \text{ W/m}^2 \quad (11)$$

$$q_{rg} = \varepsilon_g \sigma [T_g^4 - (T_o - 11)^4], \text{ W/m}^2 \quad (12)$$

The total heat loss environment, denoted as qLgq_{Lg}qLg, consists of two main components: convective heat loss (qcgq_{cg}qcg) and radiative heat loss (qrgq_{rg}qrg). The overall heat dissipation from the glass depends on both thermal radiation to the sky and convective heat exchange with the ambient air.

Radiative loss to the sky is influenced by the effective sky temperature, typically considered to be approximately 11°C lower than the ambient air temperature. The radiative component is calculated using the Stefan–Boltzmann law, where εg\varepsilon_gεg represents the emissivity of the glass and σ\sigmaσ is the Stefan–Boltzmann constant, valued at 5.67×10−8 W/m2K45.67 \,.The convective heat transfer coefficient between the glass cover and the ambient air, hcgh_{cg}hcg, can be determined using empirical correlations provided by Duffie and Beckman [9]

$$h_{cg} = 5.7 + 3.8\, w_s, \text{ W/m}^2\text{ k} \quad (13)$$

The wind speed is represented by ws.
3.2. Basin water's absorption of solar energy (qw)
Basin water's thermal energy equations are derived from Rai

[10]:

$$q_{iw} = (\tau\, \alpha)_w I - q_{Lw}, \text{ W/m}^2 \quad (14)$$

The dimensionless thermal transmissivity absorptivity of water is (τα)w, which equals 0.816.

$$q_{iw} = q_{ew} + q_{rw} + q_{cw} + q_{oil} + q_{Lb}, \text{ W/m}^2 \quad (15)$$

المجلة العراقية للبحوث الإنسانية والإجتماعية والعلمية
Iraqi Journal of Humanitarian, Social and Scientific Research
Print ISSN 2710-0952 Electronic ISSN 2790-1254

The saline water surface, represented by qewqis directly related to the **hourly yield** of distilled water (Wh). This parameter is calculated using the following expression:

$$q_{ew} = \frac{W_h \times 10^{-6} \times \rho_w \times L_w}{3600} \text{ , W/m}^2 \qquad (16)$$

where LwL_, which has a value of roughly 2.35 × 10^3 kJ/kg, stands for the latent heat of vaporization of water at the temperature of the glass cover. The following relation can be used to express the desalination system's thermal efficiency, which is amount of produced daily to the total amount of solar energy input :

$$\eta_d = \frac{W_d \times 10^{-6} \times \rho_w \times L_w}{3600 \times I} = \frac{2.35\ \rho_w W_d}{3600 \times I} \qquad (17)$$

Where WdW denotes the **total volume of distilled water collected per day** (in liters or kilograms), and III represents the **total incident** received per unit area, measured in **kJ/(m²·day)**.

The term qrwq_{rw}qrw corresponds to the **radiative heat transfer rate** between the surface of the saline water and the **inner surface of the glass cover**. This radiative exchange is governed by the Stefan–Boltzmann law and can be expressed as:

$$q_{rw} = \sigma\, F_{(w-g)} [\varepsilon_w T_w^4 - \varepsilon_g T_g^4] \text{ , W/m}^2 \qquad (18)$$

with values of **0.96** and **0.89** for water and glass, respectively. Additionally, Fw→gF represents the **radiation shape factor** between the saline water surface and the inner glass cover, which is assumed to be **0.9** in this analysis.The term qcwq_{cw}qcw denotes the **convective heat transfer rate** between the saline water surface and the inner glass cover. It is determined using the following expression:

$$q_{cw} = h_{cw} (T_w - T_g), \text{ W/m}^2 \qquad (19)$$

where, or hcw, is determined using the following formula.:

Print ISSN 2710-0952 Electronic ISSN 2790-1254

$$h_{cw} = 8.84 \times 10^{-4} \times \left(T_w - T_g\right) \times \left\{ \left(T_w - T_g\right) + \left[\frac{P_w - P_g}{2.65 * \left(P_t - P_w\right)} \right] \times T_w \right\}^{1/3}, \mathrm{W/m^2\ ^\circ C} \quad (20)$$

where, in N/m2, PwP_, PgP_, and PtP_ stand for the vapor pressure of water at the saline surface temperature, the vapor pressure at the clear glass cover's inner surface temperature, and ambient pressure, respectively.The pace at which heat energy moves from the oil to the basin water is referred to as qoil. This is the quantity of heat that is absorbed by the thermal oil that circulates inside the serpentine heat exchanger and then transferred to the saline water at the basin base via convective and conductive heat exchange processes

$$q_{\mathrm{oil}} = \left[\dot{m} C_p \left(T_{\mathrm{in}} - T_{\mathrm{out}}\right) \right]_{\mathrm{oil}} = UA\left(T_{\mathrm{in}} - T_{\mathrm{out}}\right)_{\mathrm{oil}}, \ \mathrm{W/m^2} \quad (21)$$

$$w = \dot{V}/A, \text{ where } \dot{V}\ (\mathrm{m^3/s})$$

Where **U**represents the **overall heat transfer coefficient** in units of **W/m²·°C**. Based on the pump performance curve (refer to Fig. 10), the **mass flow rate of the thermal oil** m˙\dot{m}m˙ is calculated using the equation:

m˙=ρoil·V

Given that the inlet temperature TinT_{\text{in}}, the oil's exit temperature is calculated using energy balance principles.Assuming steady-state circumstances and no heat loss in the loop, tin is known

$$T_{\mathrm{out}} = T_{\mathrm{in}} + \frac{q_{\mathrm{oil}}}{\dot{m} C_P}, \mathrm{K} \quad (22)$$

1. The heat exchanger, denoted by U (W/m²•°C), should be computed using the following assumptions, which simplify the thermal analysis:

Print ISSN 2710-0952 Electronic ISSN 2790-1254

2. The **variations in kinetic and potential energies** of the fluids are negligible and thus not included in the analysis.

3. The **heat transfer surfaces are clean**, i.e., no fouling or scaling is present, ensuring unimpeded heat exchange.

4. The **thermophysical properties** of both fluids (thermal oil and saline water) are considered **constant** throughout the operation.

5. The **thermal resistance of the heat exchanger wall** is neglected due to the **high thermal conductivity** and **thin-walled structure** of the copper tubing used.

Under these conditions, the overall heat transfer coefficient UUU can be calculated using **standard heat exchanger analysis methods**, such as or the **effectiveness-NTU** (Number of Transfer Units) method, depending on the available data and flow configuration

$$U = \frac{q_{\text{oil}}}{A\Delta T_{\text{oil}}} \quad , \text{W/m}^2\,\text{K} \qquad (23)$$

$$q_{Lb} = h_{Lb}\,(T_w - T_o),\ \text{W/m}^2 \qquad (24)$$

denoted by hLb (W/m2 K), is determined by thermal conductivity and the thickness of the insulating layer.

[10]:

$$h_{Lb} = \frac{K_{\text{in}}}{X_{\text{in}}} \quad , \text{W/m}^2\,\text{K} \qquad (25)$$

Kin and Xin, which stand for thermal conductivity and thermal insulation thickness, respectively, are 0.03W/mEC and 0.05 m.

4. Studying economics
The capital costs of the components are the main annual expenses for a desalination plant.

Table 2 Description and costs of the components of the present solar desalination systems,

Print ISSN 2710-0952 Electronic ISSN 2790-1254

Components	Specification	No. × cost (LE)	Total cost
Galvanized steel sheet, m	(1×1) m, 08 mm thickness	2 × 50	100
Still supported (H-section), m	5 m, 2 mm thickness	5 × 20	100
Glass cover, sheet	1.02 × 1.02 4 mm	1 × 75	75
Parabolic trough (solar collector), sheet	Stainless steel 314, 04 mm	1 × 300	300
Silicon rubber	Clear	3 × 10	30
Plastic tank, m^3	0.2	1 × 10	10
Parabolic trough iron stand (L-section), m	Steel skeleton with multi position sides (0° to 180°)	1 × 100	100
Valves	0.5 inch	3 × 10	30
Foam, 5 cm thickness, sheet	2 m^2	2.2 × 15	33
Glass wool insulation, m	5 m	5 × 15	75
Trough copper pipe line, m	2 m, 7/8 inch hardened copper	2 × 27.5	55
Serpentine heat exchanger copper pipe	20 m, 5/8 inch	20 × 10	200
Oil + oil small pump	Q_{max} =30 L/min, H_{max} = 28 m, 0.5 HP	1 × 225	225
Added costs	Claim of this work	50	50
Total costs of initial construction	Present system	1 × 1383	1383

5. Results and Discussion

Figures 11 to 22 illustrate the thermal performance, fresh water productivity, and cumulative daily output of both the conventional and modified solar desalination systems under the defined case study conditions.

The hourly variation of solar radiation (I) and its influence on both systems during the experimental days (April 6, 2005, and June 5, 2005) is shown. The ambient temperature (TaT_) and inner glass cover temperature (Tg) exhibit a general increase as solar intensity rises, reaching their peak values between 11:30 AM and 3:30 PM, as depicted in Figures 11 and 16.

Figures 12 and 17 show the hourly variation of basin water temperature (TwT_) in relation to ambient conditions. As the day progresses, temperatures increase, reaching their maximum in the early afternoon, before declining after 4:00 PM, in accordance with the solar radiation profile. Notably, the temperatures recorded for are consistently higher than those of the conventional system, indicating improved thermal efficiency.

Figures 13 and 18 present the temperature variation within the oil circulation loop on the selected test days, further confirming the enhanced heat transfer characteristics of the modified system

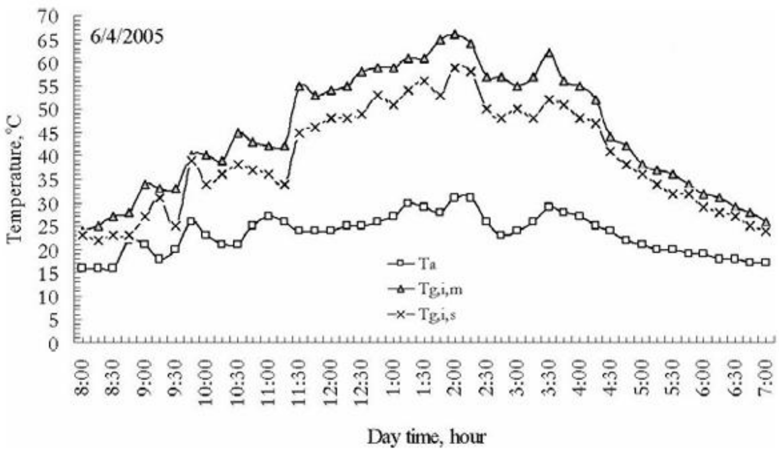

Fig. 11. Variations of ambient tem perature and inner glass temperature for standard and modified solar stills.

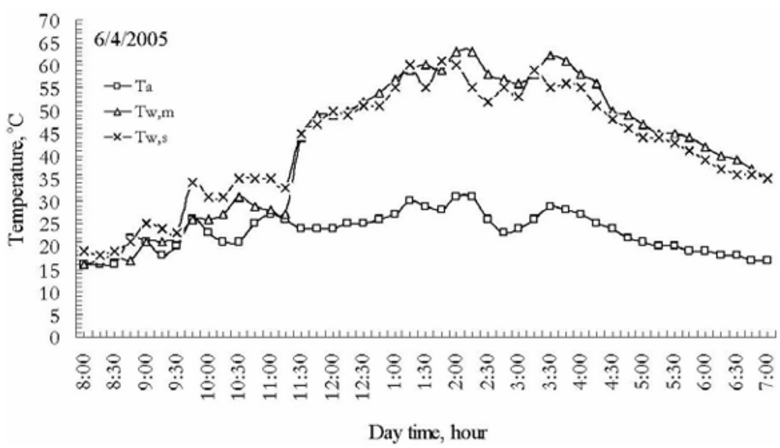

Print ISSN 2710-0952 Electronic ISSN 2790-1254

Fig. 12. Variations of ambient tem perature and basin water for standard and modified solar stills.

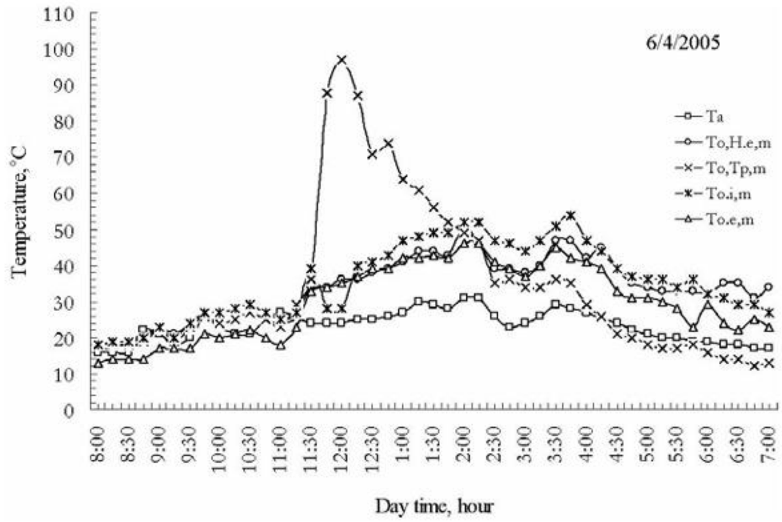

Fig. 13. Temperature variations of oil cycle

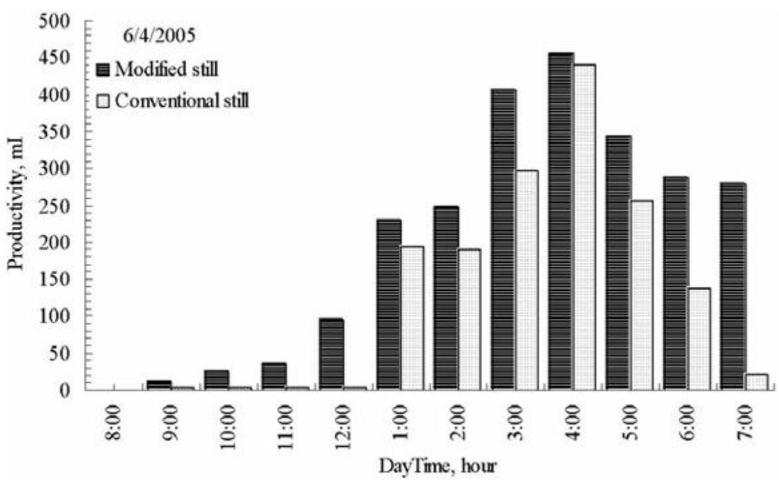

Fig. 14. Fresh water productivity for the conventional and modified solar stills

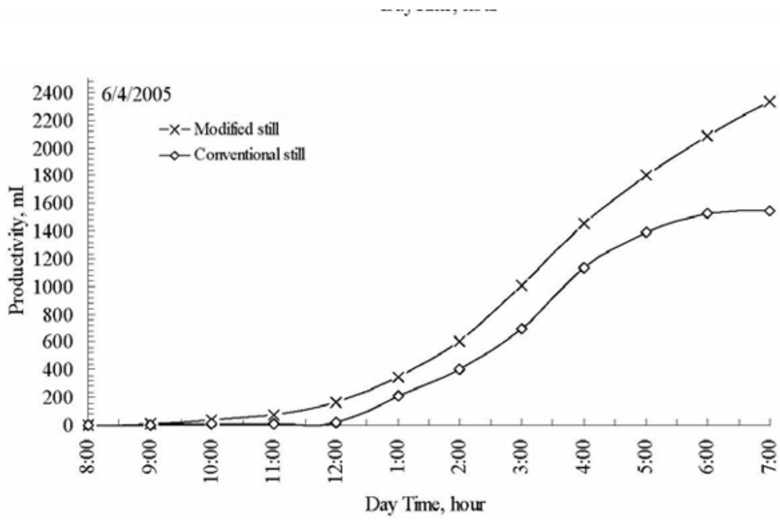

Fig. 15. Accumulative fresh water productivity for the conventional and modified solar stills

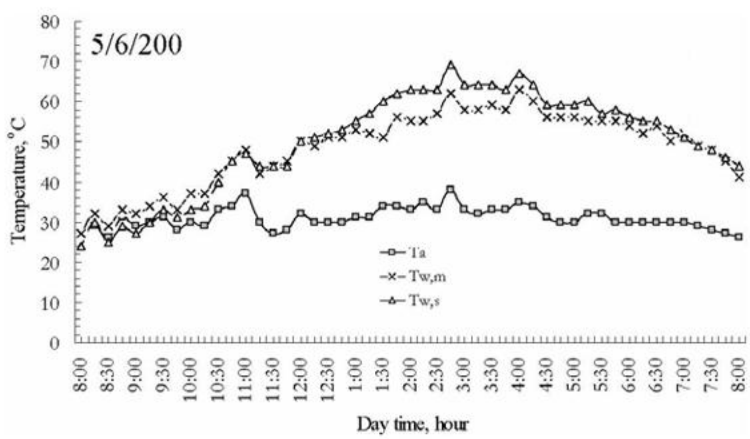

Fig. 16. Variations of ambient tem perature and inner glass temperature for standard and modified solar stills

المجلة العراقية للبحوث الإنسانية والإجتماعية والعلمية العـــدد 19A تشر2ين 2025
Iraqi Journal of Humanitarian, Social and Scientific Research No.19A Nov. 2025
Print ISSN 2710-0952 Electronic ISSN 2790-1254

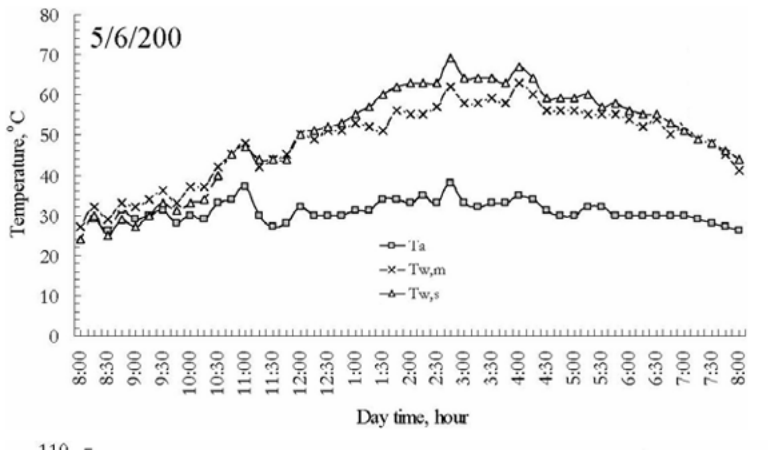

Fig. 17. Variations of ambient temperature and basin water for standard and modified solar stills.

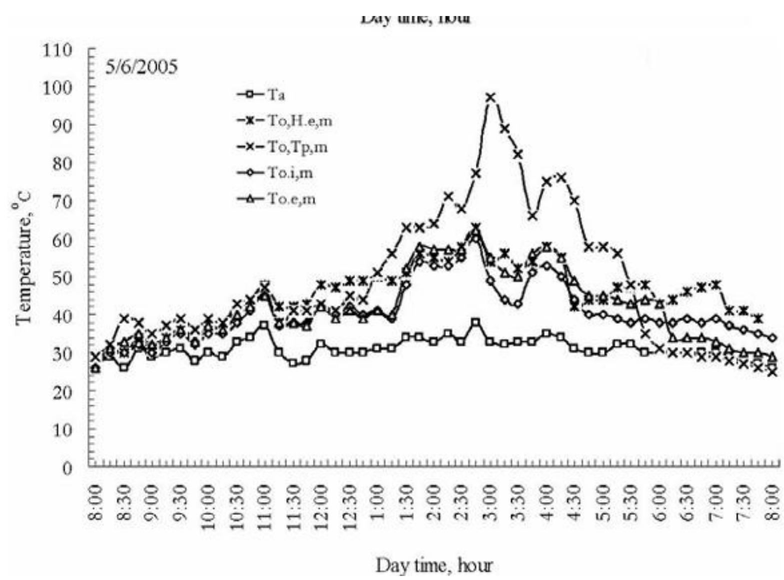

Fig. 18. Temperature variations of oil cycle

المجلة العراقية للبحوث الإنسانية والإجتماعية والعلمية
Iraqi Journal of Humanitarian, Social and Scientific Research
Print ISSN 2710-0952   Electronic ISSN 2790-1254

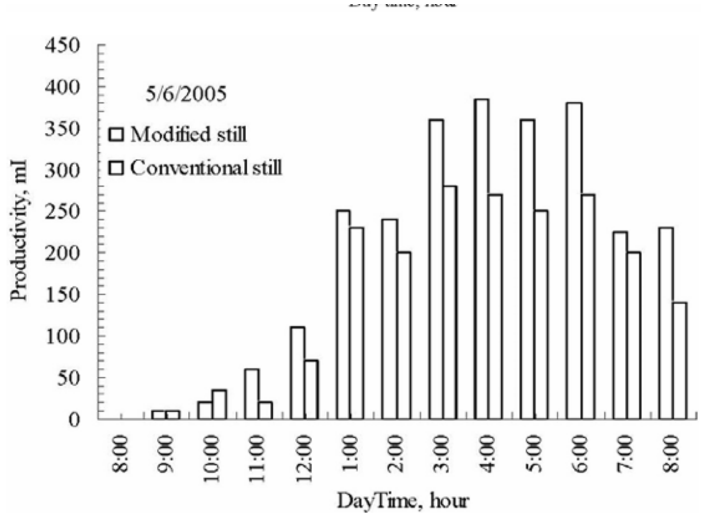

Fig. 19. Fresh water productivity of conventional and modified solar stills

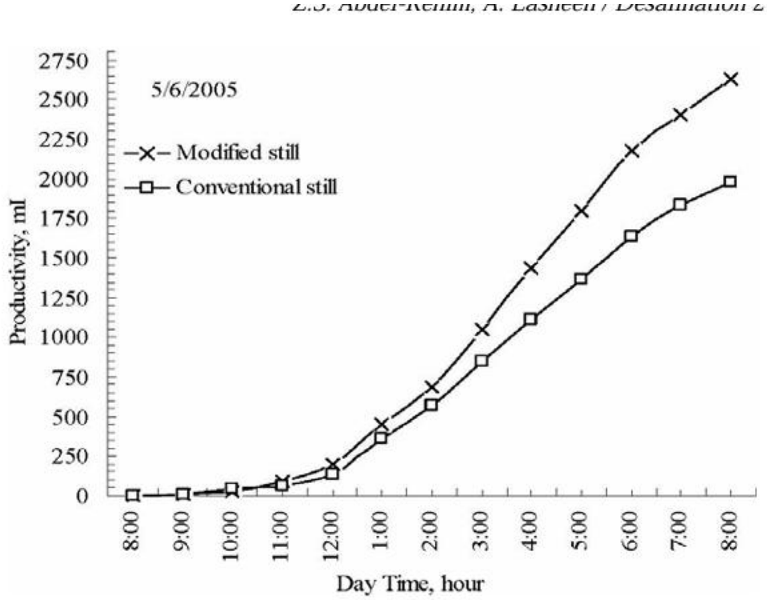

Fig. 20. Accumulative fresh water productivity of conventional and modified solar stills

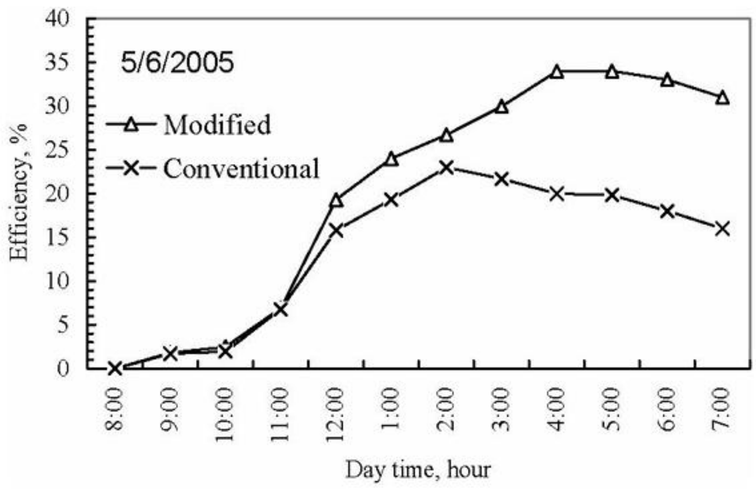

Fig. 21. Efficiency comparison be tween the conventional and modified desalination systems

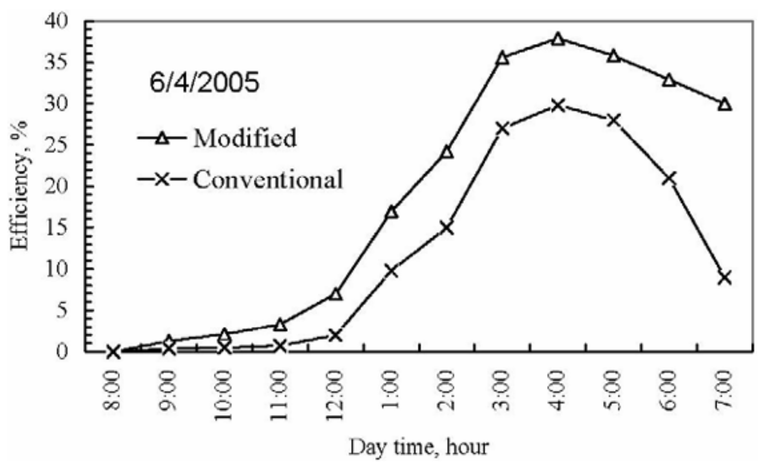

Fig. 22. Efficiency comparison be tween the conventional and modified desalination systems.

The thermal oil temperatures in the parabolic trough pipe, at the heat exchanger's intake, and inside the heat exchanger itself—which is situated at the bottom of the basin—were found to be continuously greater than the heat exchanger's exit oil temperature. The efficient passage of heat from the oil to the basin water during the heat exchange process is confirmed by this temperature disparity. The hourly fresh water productivity for the modified and traditional systems is shown in Figures 14 and 19. The information unequivocally demonstrates that the adjusted system generates noticeably more productivity all day long .

Additionally, cumulative fresh water production, presented in Figures 15 and 20, confirms that the modified system yields greater overall distilled water output compared to the conventional system.

The overall performance evaluation, illustrated in Figures 21 and 22, further supports the conclusion that the modified solar desalination system demonstrates enhanced efficiency and improved operational effectiveness

. 6. Conclusions

The study showed that as the day progresses, temperatures within the system rise and reach their peak before starting to fall after around 4:00 PM, which matches the pattern of solar radiation during the day. The modified system consistently maintained higher temperatures than the conventional system, indicating better heat retention or absorption.

The thermal oil temperatures at key points in the system—inside the parabolic trough, entering the heat exchanger, and within the heat exchanger itself—were higher. This means that heat was effectively transferred from the oil to the basin water, improving the system’s performance.The modified system also produced more fresh water both hourly and daily compared to the conventional system, showing its superior productivity.

Overall, the modifications made to the solar desalination system improved its efficiency, resulting in about an 18% increase in the amount of fresh water generated, proving the success of the design improvements

References

[1] M.S. Abu-Jabal, I. Kamiya and Y. Narasaki, Proving test for a solar-powered desalination system in Gaza Palestine, Desalination, 137 (2001) 1–6.

[2] K. Schwarzer, M.E. Vieira, C. Faber and C. Muller, Desalination, 137 (2001) 23–29.

[3] S. Al-Kharabsheh and D. Yogi Goswami, Analysis of an innovative water desalination system using low-grade solar heat, Desalination, 156 (2003) 323 332.

[4] K. Schwarzer, M.E. Vieira, H. Lehmann and L. Coutinho, Modular solar thermal desalination system with flat plate collector, Proc. Rio 3–World Climate & Energy Event, Rio de Janeiro, 2003.

[5] E.D. Howa, Distillation of seawater, in W.C. Dickinson and P.N. Cheremisionoff, eds., Solar Energy Handbook, Marcel Dekker, New York, 1980, pp. 205–237.

[6] M.M. Ghoraba, Theoretical and experimental studies of heat and mass transfer inside single sloped solar still, Ph.D. Thesis, Faculty of Engineering, Cairo University, Egypt, 1987.

[7] M. Shaltout, Egyptian Solar Radiation Atlas, Geo graphy Institute, Cairo, Egypt, 1998.

[8] W.J. Smith, Modern Optical Engineering, McGraw Hill, New York, Hill, 1966.

[9] J.A. Duffie and W.A. Backman, Solar Engineering of Thermal Processes, 2nd ed., Wiley, New York, 1991.

[10] G.D. Rai, Solar Energy Utilization, Textbook for Engineering Students, Khanna, Nai Sarak, New Delhi, India, 1980.